Strained-layer InGaAs Quantum-well Lasers Emitting beyond 2 μm

Manabu Mitsuhara[†], Takao Watanabe, and Yasuhiro Kondo

Abstract

Semiconductor lasers emitting in the mid-infrared wavelength region have attracted much attention as light sources for environmental and medical applications. We have succeeded in developing strained-layer InGaAs quantum-well lasers on InP that exhibit single-mode operation with emission wavelengths beyond 2 µm by using the technologically mature fabrication techniques of telecommunications lasers. Fabricated distributed-feedback lasers exhibit continuous wave operation in the temperature range from 15 to 55°C, emission wavelengths longer than 2.1 µm, and optical output power higher than 10 mW at 25°C. These laser characteristics are sufficient for practical light sources for laser-based spectroscopy.

1. Introduction

Mid-infrared lasers with emission wavelength of around 2 µm are very useful for trace-gas monitoring applications in environmental and medical diagnostics. This is because the first-overtone vibrational absorption lines of various gases such as CO_x and NO_x are located in this wavelength range. This laser absorption spectroscopy makes possible measurement systems that have a quick response and provide non-invasive diagnosis. For most sensor applications, tunable light sources with single-mode operation and an output power of several milliwatts are favorable. Among the mid-infrared lasers, semiconductor lasers have advantages over solid-state and gas lasers in terms of compactness, energy efficiency, and cost effectiveness. Semiconductor lasers with emission wavelengths of 2–3 µm include InP-based, Sb-based, and lead salt lasers. In comparison with the other lasers, the InP-based laser can easily achieve single-mode operation because the processing technologies are mature, as they were developed for telecommunications lasers. In addition, both superior substrate quality and technologically mature growth methods make the InP-based lasers attractive candidates for light sources in sensor applications.

For the InP-based laser, a distributed feedback (DFB) structure and a buried heterostructure are used to fix the longitudinal and transverse modes, respectively. The structure of the conventional InP-based DFB laser is shown schematically in **Fig. 1**. The structural characteristics are as follows. First-order gratings are formed on the upper InGaAsP waveguide layer and a p-InP cladding layer is regrown on the gratings. The active region, which is composed of multiple quantum-wells (MQWs), is processed into
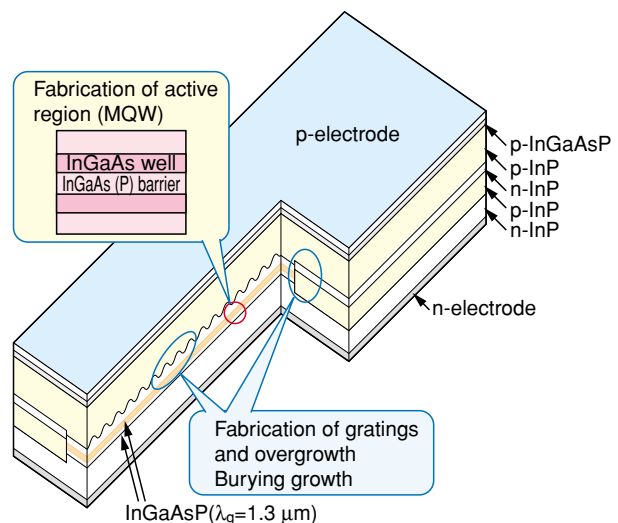

Fig. 1. Schematic structure of a typical DFB laser using InP-based materials. The active region is composed of MQWs.

† NTT Photonics Laboratories
Atsugi-shi, 243-0198 Japan
E-mail: mituhara@aecl.ntt.co.jp

mesa stripes, and then the stripes are buried with p-InP and n-InP current-blocking layers. The grating fabrication and regrowth process are well-established techniques. However, the emission wavelength of conventional InP-based DFB laser ranges from 1.3 to 1.55 μm. A DFB laser on InP emitting beyond 2 μm is difficult to fabricate because the bandgap of InP-based material corresponds to a wavelength shorter than 1.7 μm when the layer is lattice-matched to InP substrate.

NTT Photonics Laboratories has developed technology for growing high-quality strained-layer InGaAs quantum wells (QWs), which enables us to fabricate mid-infrared lasers with an emission wavelength longer than 2 μm [1], [2]. In this paper, we report our recent results for 2-μm lasers with strained MQW active regions. Section 2 describes the material properties of strained InGaAs layers grown on InP and clarifies the material parameters for obtaining a bandgap wavelength longer than 2 μm. Section 3 covers some issues in the epitaxial growth of strained-layer MQWs. Section 4 presents the device characteristics of the DFB lasers. Finally, Section 5 draws some conclusions and mentions future prospects.

2. Material properties of InGaAs
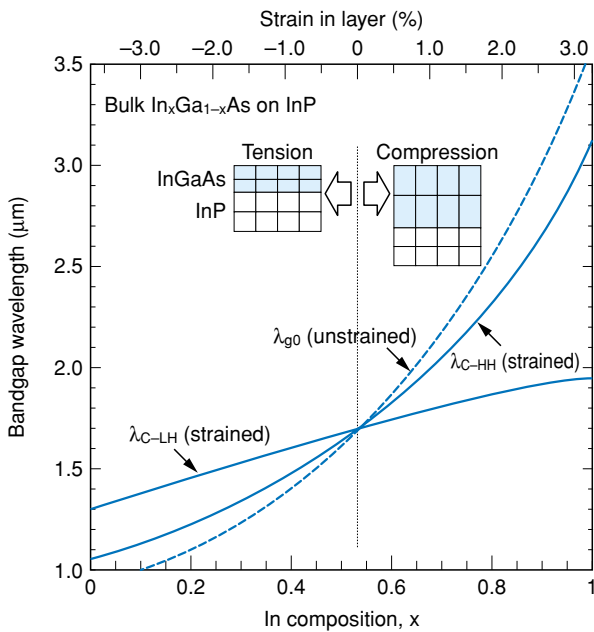
To design the laser structure, we need to know

material parameters such as the lattice constant and bandgap energy E_g for each of the constituent layers. Conveniently, the material parameters for InP-based compounds have been extensively studied for the application of these compounds as laser materials for fiber-optic communications. **Figure 2** shows the calculated bandgap wavelength (λ_g (μm) = 1.2407/E_g (eV)) for a bulk $In_xGa_{1-x}As$ layer on InP as a function of In composition. As illustrated in the inset of Fig. 2, the InGaAs layer is tetragonally distorted to accommodate the mismatch strain between it and the InP. The lattice distortion modifies the band structures and the bandgap energy. The heavy hole (HH) band is above the light hole (LH) band in the compressively strained state, whereas the LH band is above the HH band in the tensilely strained state [3], [4]. Curve λ_{g0} is the bandgap wavelength without consideration of the lattice distortion. The bandgap wavelengths with consideration of the lattice distortion are shown by curves λ_{C-HH} and λ_{C-LH}. As shown in Fig. 2, a compressive strain larger than 1% is required to obtain a bandgap wavelength longer than 2 μm. When a QW structure is used instead of a bulk layer, the bandgap wavelength becomes smaller because of the quantum size effect on the bandgap energy. Therefore, a very large strain is required for InGaAs QWs to obtain the same bandgap wavelength as bulk InGaAs.

Figure 3 shows the calculated bandgap wavelength as a function of well thickness for a strained-layer InGaAs QW sandwiched between $In_{0.53}Ga_{0.47}As$ barriers. Here, the bandgap energy is the energy of interband transition from an $n = 1$ electron (E) state to an $n = 1$ HH state. As shown in Fig. 3, obtaining a bandgap
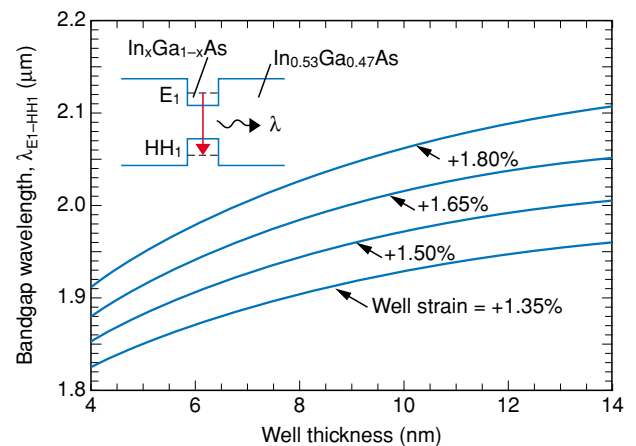
Fig. 2. Calculated bandgap wavelength for strained and unstrained $In_xGa_{1-x}As$ on InP as a function of In composition. The upper horizontal axis shows the mismatch strain of $In_xGa_{1-x}As$ with respect to InP. Insets illustrate the lattice distortion due to the mismatch strain.

Fig. 3. Calculated bandgap wavelength as a function of well thickness for an InGaAs QW sandwiched between $In_{0.53}Ga_{0.47}As$ barriers. The well strains were +1.35, +1.5, +1.65, and +1.8%. The inset shows the recombination process between electrons and holes in the QW.

wavelength longer than 2 µm requires well strain larger than +1.5%. When the well strain is increased, however, the QW layer relaxes, resulting in the generation of misfit dislocations and/or a change in the growth mode from two-dimensional (2D) to three-dimensional (3D) above a critical layer thickness [5], [6].

Here, we consider the critical layer thicknesses for InGaAs on InP based on calculations using the energy balance model with consideration of the growth-temperature dependence [7]. The calculated thicknesses for InGaAs on InP are shown in **Fig. 4**. The critical layer thickness is close to the well thickness at which the bandgap wavelength of 2 µm is obtained (Fig. 3). For example, the critical layer thickness for +1.65%-strained InGaAs at a growth temperature of 600°C is 13 nm, which is about the same as the well thickness at which the bandgap wavelength of 2.05 µm is obtained. On the other hand, decreasing the growth temperature is effective in increasing the critical layer thickness for InGaAs as shown in Fig. 4. However, for InGaAs with a large strain, the increase in the critical layer thickness with decreasing growth temperature becomes smaller. For example, the critical layer thickness for +1.5%-strained InGaAs at 400°C is 4 nm larger than that at 600°C, but decreasing the growth temperature from 600 to 400°C increases the critical layer thickness for +1.8%-strained InGaAs by only 2 nm and lengthens the bandgap wavelength by only 0.02 µm (Fig. 3). Therefore, in the wavelength region longer than 2 µm, increasing the bandgap wavelength is difficult to achieve even with a low growth temperature. In addition, decreasing the growth temperature generally
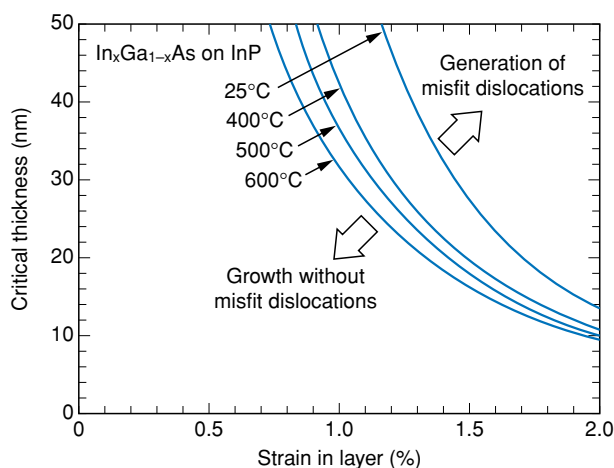
deteriorates the crystalline quality. Thus, in addition to low growth temperature, other growth conditions need to be investigated in order to fabricate strained-layer InGaAs QW lasers emitting beyond 2 µm.

3. Fabrication of strained-layer InGaAs QW

To obtain strained-layer InGaAs QW lasers with good device characteristics, we must decrease the structural defects in the active region as much as possible. For the fabrication of 2-µm MQW lasers, the active region growth must have more precise composition control of InGaAs than is necessary for 1.55-µm lasers because the well layer contains much larger strain. In addition, low-temperature growth methods are better for increasing the critical layer thickness of the strained well, as discussed in Section 2. Metalorganic molecular beam epitaxy (MOMBE) is an attractive growth method for fabricating the active region of 2-µm MQW lasers, not only for its high controllability of InGaAs composition but also for its low growth temperature. All the samples in this investigation were grown by MOMBE at a growth temperature of 510°C, which is about 100°C lower than the growth temperature of metalorganic vapor phase epitaxy (MOVPE). The well strain was varied from +1.65 to +1.9% by altering the group III fluxes, and the number of wells was four.

The room-temperature (RT) photoluminescence (PL) spectrum of the sample having +1.8%-strained InGaAs wells grown at a growth rate of 0.47 nm/s is shown in **Fig. 5** (lower dotted curve). The barrier
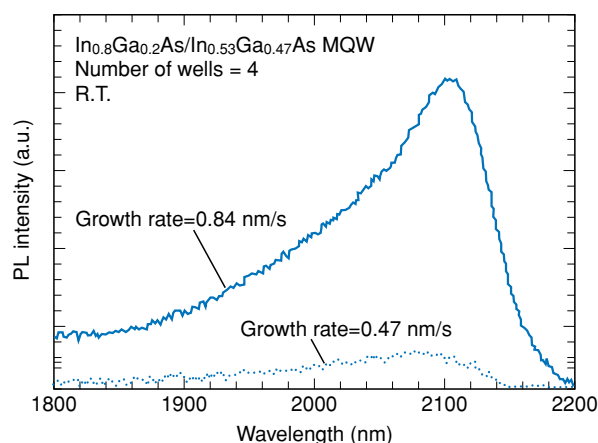

Fig. 4. Calculated critical layer thickness of InGaAs on InP for growth temperatures of 25, 400, 500, and 600°C.

Fig. 5. Room-temperature PL spectra of $In_{0.8}Ga_{0.2}As/In_{0.53}Ga_{0.47}As$ MQWs grown at well growth rates of 0.47 nm/s (lower dotted curve) and 0.84 nm/s (upper solid curve).

composition was $In_{0.53}Ga_{0.47}As$ lattice-matched to InP. The sample exhibited weak PL emission, and a rough surface was observed with a Nomarski phase contrast microscope. The decrease in PL intensity indicates the generation of structural defects that act as nonradiative recombination centers. Because large elastic stress in strained InGaAs on InP easily induces 3D island growth [5], the weak PL emission can be explained by strain relaxation through 3D island dislocations. Increasing the growth rate is effective in suppressing the 3D growth of strained film [8]. The PL spectrum obtained from the sample grown with the high growth rate (0.84 nm/s) is shown in Fig. 5 (upper solid curve). The PL peak wavelength at 2.1 μm was about the same as that for the sample grown with the low growth rate (0.47 nm/s). In contrast, the PL peak intensity was increased tenfold by increasing the growth rate. In addition, the high-growth-rate sample had a specular surface. By increasing the growth rate of the well layer, we could obtain an

MQW containing +1.8%-strained InGaAs wells without decreasing the PL intensity.

The net strain of a strained-layer MQW can be reduced by making the barrier layers strained in the opposite sense to the well strain; this is generally called the strain-compensated technique. Here, the net strain ε^* is given by $\varepsilon^* = (\varepsilon_w L_w + \varepsilon_b L_b) / (L_w + L_b)$, where ε_w, L_w, ε_b, and L_b are well strain, well thickness, barrier strain, and barrier thickness, respectively.

Next, we studied the effect of the barrier strain on the structural and optical properties of the strained-layer MQW [9]. The strain and thickness of the well layer were kept constant at +1.65% and 11.5 nm, and the net strain was altered by the strain of the barrier layer. **Figure 6(a)** plots the PL peak intensity versus barrier strain. The upper horizontal axis shows the net strain. The samples had a large PL peak intensity for barrier strain ranging from –0.17 to +0.14%, which is close to the lattice-matching condition. In contrast,
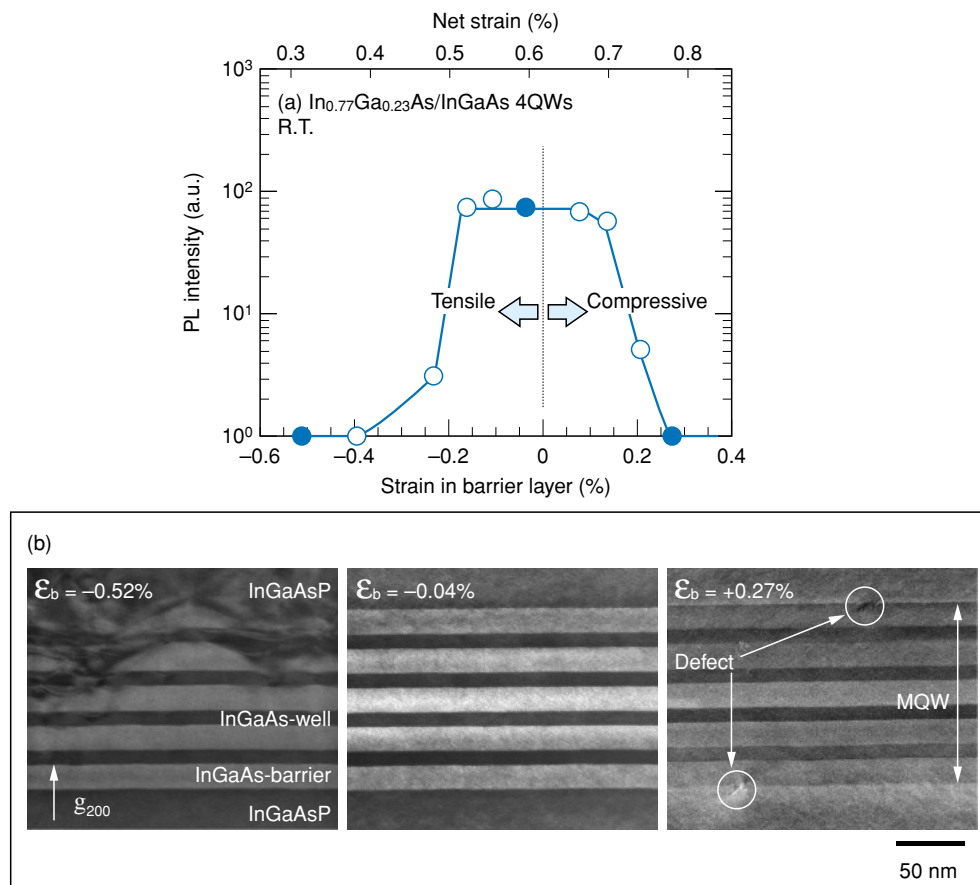

Fig. 6. (a) Plot of the PL peak intensity of $In_{0.77}Ga_{0.23}As/In_{0.53}Ga_{0.47}As$ MQWs versus the strain in the barrier layer and (b) cross-sectional TEM photographs of MQWs for barrier strains of –0.52, –0.04, and +0.27%. The micrographs were taken with a diffraction vector $g = 200$.

the PL peak intensity decreased by as much as two orders of magnitude when the barrier strain was outside this range. It should be noted that the samples with the barrier strain smaller than –0.23% exhibited weak PL emission in spite of the small net strain. The PL degradation indicates that nonradiative recombination centers were introduced into the MQW, as mentioned before. **Figure 6(b)** shows cross-sectional transmission electron microscope (TEM) photographs of MQWs with barrier strains of –0.52, –0.04, and +0.27%. For the sample with –0.52%-strained barriers, the well and barrier layers had thickness undulations, and structural defects were generated at the undulations. In the case of –0.04%-strained barriers, the interfaces between the well and barrier layers were flat and no defects were seen. The sample using +0.27%-strained barriers also exhibited flat interfaces between the well and barrier layers, but a pair of defects can be seen in the top and bottom interfaces between the MQW and the InGaAsP waveguide layers. From a comparison of Figs. 6(a) and (b), it is clear that the effective barrier-layer condition is close to lattice-matching. Consequently, it is difficult to apply the strain-compensation technique to strained-layer InGaAs MQWs used as the active regions of 2-µm lasers.

By combining the increase in well layer growth rate with barrier strain adjustment, we were finally able to obtain InGaAs MQWs with a well strain larger than +1.9% without any degradation of the crystalline quality.

4. Device fabrication and characteristics

The fundamental processes for fabricating 2-µm DFB lasers are well established, as mentioned in Section 1. We fabricate the DFB lasers as follows. First, the active region composed of a separate-confinement-heterostructure MQW is grown at 510°C by MOMBE. The MQW active region consists of four InGaAs wells and five $In_{0.53}Ga_{0.47}As$ barriers, where the well strain is adjusted to obtain PL peak wavelengths of 2.05 and 2.1 µm. Next, the first-order gratings are fabricated on the upper InGaAsP waveguide layer using electron beam lithography and wet etching. This is followed by a three-step regrowth process using MOVPE at the growth temperature of 600°C. Specifically, a p-InP cladding layer is first grown on the gratings. Next, 1.5-µm-wide mesa stripes are formed on the wafer, and then p-InP and n-InP current blocking layers are grown around the mesa stripes. Finally, a p-InP cladding layer and a p-
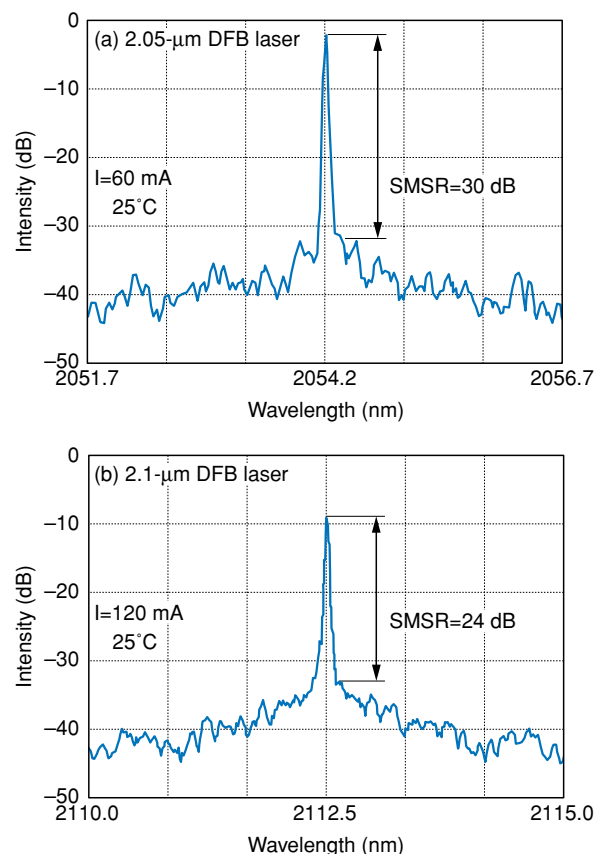

Fig. 7.   Emission spectra of (a) 2.05-µm and (b) 2.1-µm DFB lasers under CW operation at 25°C.

InGaAs contact layer are grown on the wafer after removal of the mesa-defining SiO_2 mask. After contact metallization, the wafer is cleaved into bars with cavity lengths of 600 and 900 µm.

Figures 7(a) and **(b)** show the emission spectra of the DFB lasers with Bragg wavelength of 2.05 and 2.1 µm. The emission wavelengths of the DFB mode are 2.0542 and 2.1125 µm, respectively, which agree quite well with the designed Bragg wavelengths. The emission wavelength of 2.1125 µm is the longest ever reported for InP-based DFB lasers using interband transitions between the conduction and valence bands. For both lasers, the side-mode suppression ratio (SMSR) was higher than 24 dB, which is sufficient for light sources of sensor applications.

For practical use in trace-gas monitoring application, the emission wavelength of the light source must be tunable over a range of several nanometers. **Figure 8** shows the relationship between the emission wavelength of the 2.05-µm DFB laser and the injection current for various heatsink temperatures. The cavity length of the DFB laser was 900 µm. The emission

wavelength of the DFB laser changed from 2.051 to 2.056 µm as the heatsink temperature was increased from 15 to 55°C. The wavelength shift with increasing temperature was fairly constant at 0.125 nm/°C, which is about the same as that of the 1.55-µm DFB laser. This indicates that the emission wavelength of the DFB laser is mainly determined by the refractive index, which means that it can be well controlled by the periodicity of the grating, in the same way that it can be for a 1.55-µm DFB laser. On the other hand, the current-tuning rate of the wavelength was almost constant at 0.0025 nm/mA in the temperature range of 15–45°C and that at 55°C was also constant at –0.002 nm/mA. Such constant tuning rates enable the emission wavelength to be finely controlled.

Applications using laser spectroscopy require not only single-mode operation but also high output power. **Figure 9** shows the continuous-wave (CW) light output power of the DFB laser versus injected current at heatsink temperatures from 15 to 55°C. The threshold current density was 26 mA at 25°C and the characteristic temperature (T_0) was measured as 50 K. These values are comparable to those of the 1.55-µm DFB laser [10]. The output power at an injection current of 200 mA was as high as 10.5 mW at 25°C and 4.1 mW even at 55°C. Such an output power is suitable for light sources in spectroscopic applications [11].
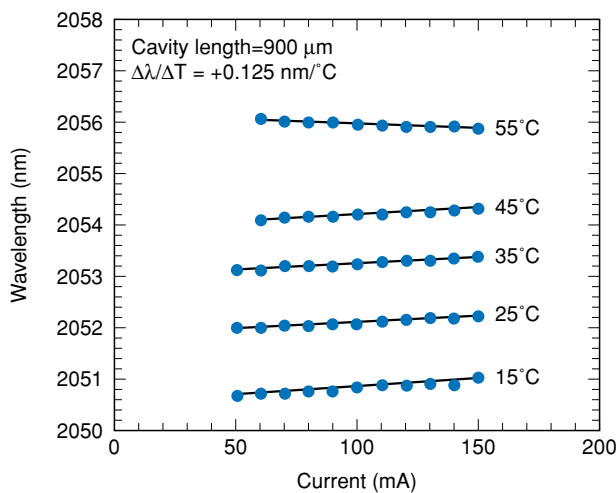
5. Conclusion and future prospects

We have demonstrated high-performance DFB lasers with emission wavelengths longer than 2 µm using strained-layer InGaAs MQWs on InP as active regions. First, we clarified that the InGaAs conditions needed to obtain a bandgap wavelength longer than 2 µm are difficult to achieve because of structural defects arising from the large well strain. By combining an increase in well layer growth rate with barrier strain adjustment, we obtained PL emission from InGaAs MQWs at wavelengths as long as 2.1 µm without any decrease in PL intensity. The fabricated DFB lasers exhibited CW single-mode operation at heatsink temperatures from 15 to 55°C. Emission wavelengths longer than 2.1 µm were obtained, and we found that the wavelength could be easily tuned by altering the injection current and heatsink temperature. The output power was higher than 10 mW at 25°C, which is sufficient for practical light sources of laser absorption spectroscopy.

For strained-layer InGaAs QW lasers, it is difficult to increase the emission wavelength further because a large mismatch strain in the well induces 3D island growth. To increase the emission wavelength without increasing the mismatch strain, researchers are looking at InGaAsN as a well material [12], [13] because adding small amounts of nitrogen causes large

Fig. 8. Emission wavelength of the DFB mode as a function of injection current for heatsink temperatures ranging from 15 to 55°C.
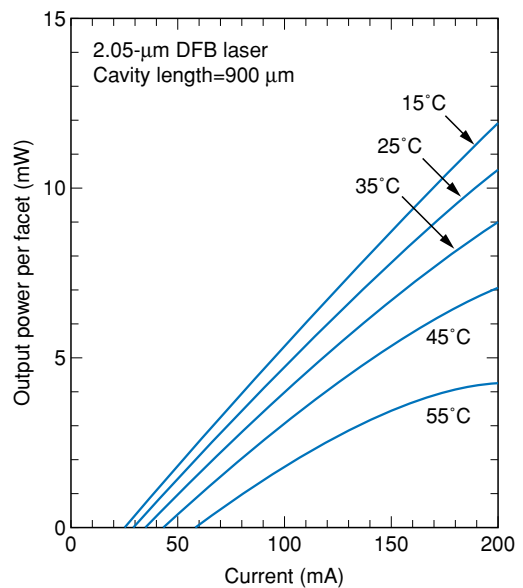
Fig. 9. CW output power versus current characteristics of the 2.05-µm DFB laser for heatsink temperatures ranging from 15 to 55°C.

bandgap bowing in the InP-based material. The use of InGaAsN wells is expected to further increase the emission wavelength of InP-based MQW lasers.

References

[1] M. Mitsuhara and M. Oishi, "2-µm wavelength lasers employing InP-based strained-layer quantum wells," in "Long-wavelength infrared semiconductor lasers (ed. H. K. Choi)," Wiley, New Jersey, pp. 19-68, 2004.

[2] M. Mitsuhara, M. Ogasawara, M. Oishi, H. Sugiura, and K. Kasaya, "2.05-µm wavelength InGaAs/InGaAs distributed-feedback multi-quantum-well lasers with 10-mW output power," IEEE Photon. Technol. Lett., Vol. 11, pp. 33-35, 1999.

[3] H. Asai and K. Oe, "Energy band-gap shift with elastic strain in $In_xGa_{1-x}P$ epitaxial layers on (001) GaAs substrates," J. Appl. Phys., Vol. 54, pp. 2052-2056, 1983.

[4] S. L. Chuang, "Efficient band structure calculations on strained quantum wells," Phys. Rev. B, Vol. 43, pp. 9649-9661, 1991.

[5] M. Gendry, V. Drouot, C. Santinelli, and G. Hollinger, "Critical thicknesses of highly strained InGaAs layers grown on InP by molecular beam epitaxy," Appl. Phys. Lett., Vol. 60, pp. 2249-2251, 1992.

[6] J. Tersoff and F. K. LeGoues, "Competing relaxation mechanisms in strained layers," Phys. Rev. Lett., Vol. 72, pp. 3570-3573, 1994.

[7] K. Kim and Y. H. Lee, "Temperature-dependent critical layer thickness for strained-layer heterostructures," Appl. Phys. Lett., Vol. 67, pp. 2212-2214, 1995.

[8] N. Grandjean, J. Massies, M. Leroux, J. Leymarie, A. Vasson, and A. M. Vasson, "Improved GaInAs/GaAs heterostructures by high growth rate molecular beam epitaxy," Appl. Phys. Lett., Vol. 64, pp. 2664-2666, 1994.

[9] M. Mitsuhara, M. Ogasawara, M. Oishi, and H. Sugiura, "Metalorganic molecular-beam-epitaxy-grown $In_{0.77}Ga_{0.23}As$/InGaAs multiple quantum well lasers emitting at 2.07 µm wavelength," Appl. Phys. Lett., Vol. 72, pp. 3106-3108, 1998.

[10] T. Tanbun-Ek, R. A. Logan, S. N. G. Chu, A. M. Sergent, and K. W. Wecht, "Effects of strain in multiple quantum well distributed feedback lasers," Appl. Phys. Lett., Vol. 57, pp. 2184-2186, 1990.

[11] R. U. Martinelli, R. J. Menna, and D. E. Cooper, "InGaAsP/InP distributed-feedback lasers for spectroscopic applications," Annual Meetings IEEE/LEOS, Boston, Massachusetts, pp. 95-96, 1994.

[12] M. R. Gokhale, J. Wei, H. Wang, and S. R. Forrest, "Growth and characterization of small band gap (~0.6 eV) InGaAsN layers on InP," Appl. Phys. Lett., Vol. 74, pp. 1287-1289, 1999.

[13] D. Serries, T. Geppert, P. Ganser, M. Maier, K. Kohler, N. Herres, and J. Wagner, "Quaternary GaInAsN with high In content: Dependence of band gap energy on N content," Appl. Phys. Lett., Vol. 80, pp. 2448-2450, 2002.

Manabu Mitsuhara
Research Engineer, Extra Long Wavelength Laser Development Project, NTT Photonics Laboratories.
He received the B.E. and M.E. in applied physics and the Ph.D. degree in engineering from Osaka University, Suita, Osaka in 1989, 1991, and 2000, respectively. In 1991, he joined NTT Optoelectronics Laboratories. From 2000 to 2003, he worked for new business development in the area of e-Learning at NTT Communications Corporation. He is currently engaged in R&D of semiconductor photonic devices. He is a member of the Japan Society of Applied Physics (JSAP).

Takao Watanabe
Senior Research Engineer, Extra Long Wavelength Laser Development Project, NTT Photonics Laboratories.
He received the B.S., M.S., and Ph.D. degrees in physics from Tokyo Institute of Technology, Tokyo in 1980, 1982, and 1995, respectively. In 1982, he joined the Electrical Communication Laboratories, Nippon Telegraph and Telephone Public Corporation (now NTT), Tokyo. Since 2001, he has been working on developing semiconductor lasers. He is a member of the Physical Society of Japan and JSAP.

Yasuhiro Kondo
Senior Research Engineer, Supervisor, Project Leader, Extra Long Wavelength Laser Development Project, NTT Photonics Laboratories.
He received the B.S. degree in physics from Kumamoto University, Kumamoto in 1984, and the M.S. and Ph.D. degrees in physics and electronic device engineering from Kyushu University, Fukuoka in 1986 and 1999, respectively. In 1986, he joined NTT Laboratories, where he has been engaged in research on MOVPE growth of III-V semiconductors and development of semiconductor lasers. He is a member of the IEEE Lasers and Electro-Optics Society and JSAP.